

Real-time Adaptation of Deep Learning Walking Speed Estimators Enables Biomimetic Assistance Modulation in an Open-Source Bionic Leg

Jairo Maldonado-Contreras, Cole Johnson, Sixu Zhou, Hanjun Kim, Ian Knight, Kinsey R. Herrin, and Aaron J. Young, *Senior Member, IEEE*

Abstract— This study introduces a real-time continual learning algorithm that incrementally improves the performance of deep-learning-based, user-independent (IND) walking speed estimators during level-ground walking with a powered knee-ankle prosthesis. Although user-dependent (DEP) estimators outperform IND estimators, they require the collection of offline, labeled DEP data. Our algorithm adapts IND Temporal Convolutional Network estimators to self-labeled DEP data and biomimetically scales prosthetic assistance based on estimated walking speed in real-time. We evaluated our algorithm on novel subjects (N=10) with unilateral above-knee amputations during treadmill and overground walking. For treadmill walking, when adapted with estimated and ground truth walking speed labels, estimators achieved mean absolute errors (MAEs) of 0.074 [0.023] (mean, [standard deviation]) and 0.074 [0.018] m/s, respectively, reflecting a 28% significant ($p < 0.05$) reduction in MAE compared to non-adapted estimators. For overground walking, estimators adapted with ground truth labels on a treadmill demonstrated an 18% significant ($p < 0.05$) reduction in MAE compared to non-adapted estimators. Our algorithm significantly reduced walking speed estimation errors within just one minute of walking and delivered biomimetic assistance ($r = 0.91$) across speeds. This approach enables off-the-shelf powered prostheses to adapt to novel users and provide appropriate assistance by accurately tracking the user's walking speed.

Index Terms— Lower-limb prostheses, Machine learning, Continual learning, Adaptive algorithms, Locomotion

I. INTRODUCTION

INDIVIDUALS with unilateral lower-limb amputations compensate for limb loss by increasing net joint moments and powers on their intact limb, compared to able-bodied

individuals [1]. Asymmetries between affected and intact limbs are exacerbated across different walking speeds [2], [3]. These compensatory behaviors may lead to secondary complications, such as increased energy expenditure [4], osteoarthritis, and back pain [5]. These effects can be mitigated with proper prosthetic fit, alignment, and device selection [5]. Specifically, devices such as semi-active and powered prostheses hold immense potential for reducing compensatory behaviors and their associated complications because they can electronically modulate assistance to closely mimic able-bodied kinematics and kinematic across speeds [6].

The C-LEG (C-LEG, Otto Bock), a semi-active, electronically controlled knee prosthesis, is programmed to vary assistance (i.e., hydraulic resistance) based on estimated cadence – a measure closely linked to speed. Across speeds, improvements in lower-limb joint kinetics [7] and step length symmetry [8] were achieved with the C-LEG compared to a passive knee prosthesis. A comparison between a mechanically controlled hydraulic knee prosthesis (3CI, Otto Bock) and the C-LEG showed that the speed-adaptive control of the C-LEG reduced metabolic expenditure at slow and medium speeds [9]. These findings highlight the significance of providing speed-adaptive assistance at varying speeds and emphasize the need for precise speed estimation.

Implementing speed-adaptive control in powered prostheses [10], [11], [12], [13] holds immense potential for benefit, as these devices can produce both propulsive and resistive assistance at the knee and ankle with electric actuation. Powered prosthesis control, typically dictated by position [11], [14], torque [15], or impedance [16], [17], can be defined by able-bodied biomechanics [14], [15] or manual tuning by experimenters [16], [17]. It can be applied discretely or continuously across speeds. Discrete control divides the gait cycle into discrete states and defines state-specific (e.g., speed-specific) behavior using finite-state machines [16]. Continuous control tracks user progression through the gait cycle and applies control trajectories that are computed from able-bodied variable-speed data [14] or invariant behaviors (i.e., intact limb movement) that do not require speed information [11]. In this study, powered prosthesis control was

Manuscript submitted #####. Asterisk indicates corresponding author. This work was supported in part by the Ford Foundation Fellowship, by a U.S. Department of Defense grant through the CDMRP Award Number W81XWH-21-1-0686, and National Institutes of Health Director's New Innovator Award No. DP2-HD111709.

*J. Y. Maldonado-Contreras, S. Zhou, H. Kim, K. R. Herrin, and A. J. Young were with the Mechanical Engineering Department, Georgia Institute of Technology, Atlanta, GA 30332 USA and with the Institute of Robotics and Intelligent Machines, Georgia Institute of Technology, Atlanta, GA 30332 USA (e-mail: jairoye@gatech.edu).

C. J. Johnson and I. Knight were with the School of Computer Science, Georgia Institute of Technology, Atlanta, GA 30332 USA.

implemented using an impedance-based finite-state machine which continuously scaled impedance parameters based on speed – enabling biomimetic behavior that can be manually tuned to user preference.

Numerous methodologies have been explored for speed estimation. These approaches can be broadly categorized into direct integration [18], [19] kinematic modeling [19], [20], [21] and machine learning methods [22]. Direct integration methods integrate foot [18] or shank [19] inertial measurement unit (IMU) linear accelerations into positional displacements that are tracked between mid-stance gait events. Speed is computed by dividing positional displacement by elapsed time. Drift error caused by signal integration is mitigated using zero velocity updates during mid-stance. Kinematic modeling methods make use of an inverted pendulum model and known limb lengths to track the progression of the user through space. Direct integration and kinematic modeling methods have achieved errors as low as 0.036 m/s RMSE for able-bodied individuals [21] and 0.09 m/s RMSE for individuals with transfemoral amputation [20]. While accurate, direct integration and traditional kinematic methods are limited to one speed estimate per gait cycle which is too slow to track immediate changes in speed. Phase-based kinematic methods are more continuous, but still require user-dependent (DEP) limb length information [21]. Machine learning methods offer a continuous and completely user-independent (IND) solution. IND solutions are preferred over DEP solutions because they can be applied out-of-the-box without any external intervention. Machine learning methods use pre-trained regression models to make continuous estimates of speed with real-time sensor data. In offline analyses, IND models (i.e., models trained on non-target subject data and evaluated on target subject data) and DEP (i.e., models trained and evaluated on target subject data) models achieved offline errors of 0.07 and 0.014 m/s RMSE, respectively. Similar disparities in IND and DEP performance have been observed in mode classification [23], slope estimation, and stair height estimation [24]. Given that the accuracy of machine-learning-based speed estimation is significantly challenged by intersubject variability, it is important to train models with DEP data to match or exceed the performance of direct integration and kinematic modeling methods. However, DEP data collection is time-consuming, often requiring several hours or days in a clinical setting to collect sufficient data. Furthermore, the need for repeated sessions for fine-tuning, as walking patterns evolve over time, renders DEP data collection impractical for many individuals. Therefore, a solution is pertinent that neither compromises model performance nor requires users to undergo impractical in-person data collections prior to use.

A promising solution to this data problem is the adoption of a continual learning strategy that adapts an IND model with self-labeled, DEP data in real-time to improve its performance

[25], [26]. This strategy was first investigated in lower-limb prostheses by Spanias et al., with the aim of continuously updating an IND mode classifier (forward classifier) with DEP electromyography data to improve classification accuracy [26]. DEP data was self-labeled using a separate classifier referred to as a backward classifier. Over time, the system adapted and enabled new EMG data to be used by the forward classifier for real-time mode classification. The adapted classifier achieved a 6.66% reduction in classification error across multiple experimental sessions when compared to the non-adapted classifier. In a related study, a Feedforward Neural Network (FNN) was used as the forward classifier and was directly adapted with labels generated by a separate FNN-based backward classifier which had access to noncausal data [25]. The aim of the study was to directly compare the performance of adapted forward classifiers, which began as IND or DEP, and non-adapted forward classifiers that were either IND or DEP. Adapting IND forward classifiers achieved errors that were not significantly different than those achieved with DEP forward classifiers. This approach is beneficial as it enables less-accurate IND classifiers to achieve performance levels comparable to DEP classifiers, making them more usable in real-world applications.

In this paper, we extend these continual learning approaches from mode classifiers to speed estimators. We also propose a novel deep-learning-based forward estimator, direct-integration-based backward estimator, and a conditional continual learning framework to improve speed estimation performance for novel subjects. Also, we implement semi-continuous speed-adaptive control to provide biomimetic assistance to subjects across speeds. Building upon the offline results presented in Johnson et al. [27] we hypothesize that our pipeline will produce adapted forward estimators that yield significantly lower real-time estimation errors compared to non-adapted forward estimators in treadmill and overground settings. Also, we hypothesize that our speed-adaptive control will achieve ankle and knee biomechanics that scale similarly ($r > 0.8$) to able-bodied biomechanics.

II. METHODOLOGY

A. Participants

Our study consisted of ten subjects with transfemoral amputations (7 males and 3 females) with an average age of 42.40 [12.70] years, height of 1.69 [0.10] m, and body weight of 71.44 [14.46] kg. All participants provided written informed consent before they participated in this study. This study was approved by the Georgia Institute of Technology IRB. A certified prosthetist configured the prosthetic device for each subject to ensure appropriate alignment and comfort.

B. Materials

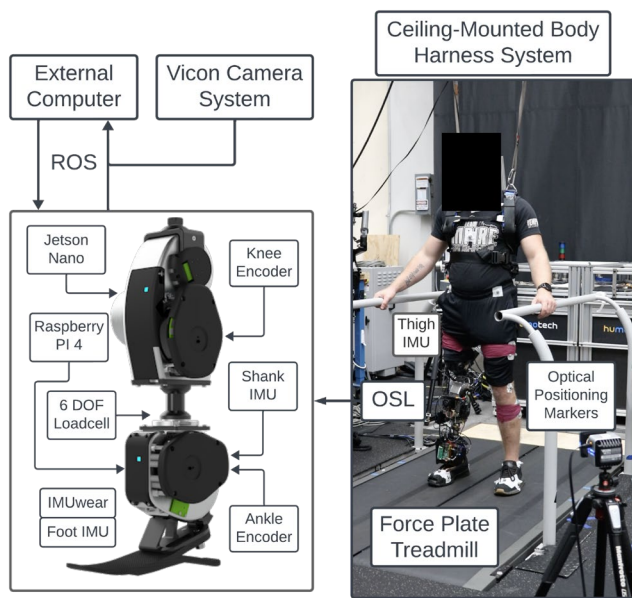


Fig. 1. Powered prosthesis, embedded sensors, and data collection equipment. Individuals with above-knee amputations walked using a powered prosthesis equipped with joint encoders, inertial measurement units, and a 6-DOF load cell. An NVIDIA Jetson Nano served as the primary computing platform that managed prosthetic control. Data were communicated over the Robot Operating System (ROS). A variable-speed Bertec instrumented treadmill was used for treadmill walking trials, and a VICON motion capture system was employed to track center-of-mass speed during overground walking.

The knee-ankle powered prosthesis used in this study was the Open-Source Leg (OSL) [10]. Our version of the OSL was equipped with one six degree-of-freedom (DOF) load cell (Sunrise Instruments M3564F, Nanning, China), two joint encoders (AS5047P & AK7452 - DEPHY Actpack, Maynard, MA), and a shank IMU (MPU-9250 InvenSense, San Jose, CA). We added two six-degree-of-freedom (DOF) Microstrain IMUs (3DMCX5-25 LORD Microstrain, Williston, VT) to the thigh and foot and a distance tracking sensor, named Imuwear (RT-BLE-001 Imuwear, Navigation Solutions LLC, Ann Arbor, MI), to the foot. A Raspberry Pi 4 imaged with a 32-bit Raspberry Pi OS was mounted on the OSL ankle housing to interface with the Imuwear sensor. An NVIDIA Jetson Nano, located on the OSL knee housing, interfaced with the Microstrain IMUs and DePHY actuators via universal serial bus. The DePHY actuators consolidated and communicated load cell, encoder, and shank IMU signals to the Jetons Nano. The Jetson Nano served as the primary computing platform of the system. An external laptop was used for signal visualization, control parameter tuning, and adaptation. All sensors were sampled at 100 Hz. Forward estimators used a total of 28 sensor channels, excluding Imuwear channels. These included 6 channels per IMU (3-axis accelerometer and gyroscope), two channels per encoder (angular position and velocity), and 6 channels for the load cell (3-axis force and moment). The Robot Operating System (ROS) enabled

wireless communication between devices.

Motion capture data were collected at 200 Hz using a 30-camera Vicon system (Vicon Industries, Inc., Hauppauge, NY). The position of four pelvis VICON markers were recorded to track center-of-mass speed, which was used as a post-hoc ground truth reference during overground walking along a 5-meter path. During treadmill walking, subjects walked on a Bertec split-belt treadmill, and treadmill speeds were communicated over ROS at 50 Hz.

C. Prosthetic Control

Prosthetic control plays a crucial role in enabling individuals with transfemoral amputations to walk naturally and adjust to varying speeds. This study presents a novel approach to prosthetic control that combines forward estimation, backward estimation, and real-time adaptation to improve speed estimation performance and deliver biomimetic assistance. Forward estimators use causal information from sensor data to estimate instantaneous speed in real-time, while backward estimators leverage noncausal information to provide more accurate speed estimates retrospectively. The prosthetic control system adapts forward estimators to an individual's walking patterns through periodic re-training with data labeled by a backward estimator. Biomimetic assistance is achieved through a finite-state machine that dictates gait phase transitions and applies joint-specific impedance parameters that scale with estimated speed. This comprehensive approach aims to provide responsive, personalized, and speed-adaptive prosthetic control for improved walking performance across various speeds.

Forward Estimation: A Temporal Convolutional Network (TCN) was selected as our forward estimator. TCNs are well-suited for real-time estimation tasks involving sequential time series data, as they can learn feature representations from long input sequences without requiring hand-engineered features [28]. TCNs have recently shown success in estimating biological joint moments in real-time [29], and we have found that they outperform more standard deep learning approaches such as CNNs and LSTMs for time-sequence biological data.

An offline dataset of variable-speed walking data, collected from eleven individuals with transfemoral amputations using the OSL [30], was used to optimize TCN hyperparameters for the task of IND speed estimation. Specifically, we optimized forward estimators with an 11-fold leave-one-subject-out cross-validation approach. The optimization process involved tuning hyperparameters such as the number of levels, channels per hidden layer, kernel size, dropout probability, and learning rate. The final optimized architecture consisted of 5 kernel size, 0.2 dropout probability, 4 levels, 10 channels per hidden layer, and a 0.0001 learning rate. The optimized input sequence length was 120 samples (1.2 seconds). This set of hyperparameters is a unique contribution of this paper which can be extended to other applications requiring real-time IND speed estimation.

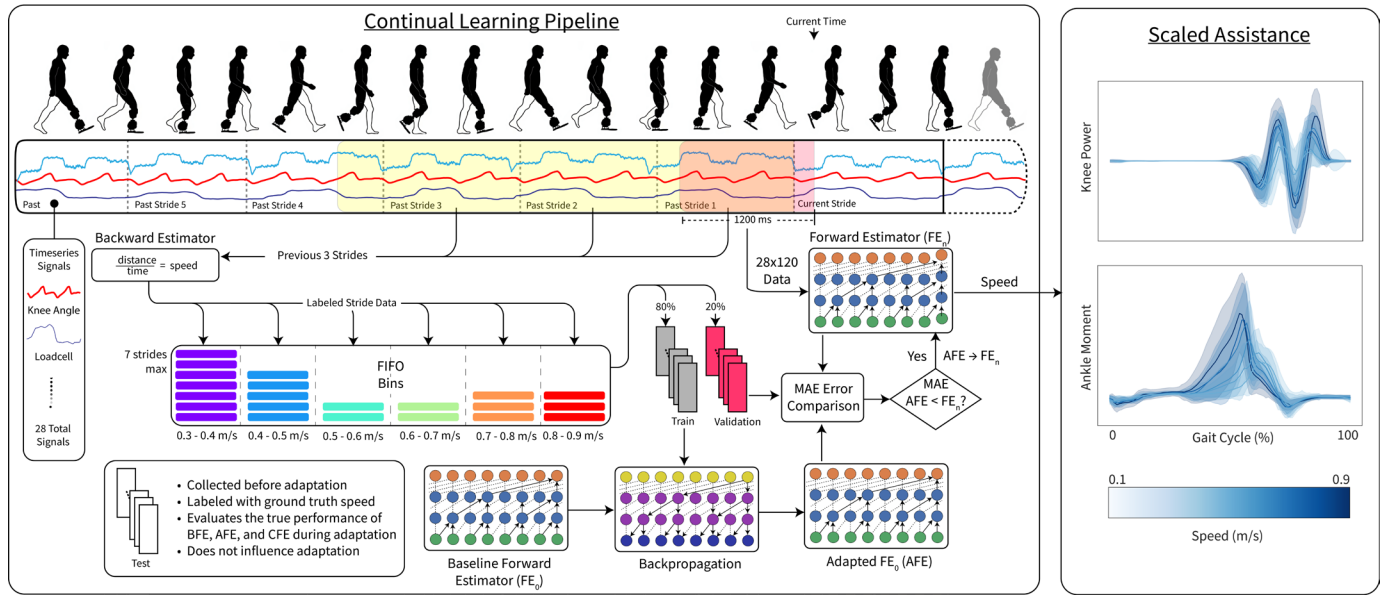


Fig. 2. Overview of the continual learning walking speed pipeline. A pre-trained, user-independent Temporal Convolutional Network walking speed regression model (baseline forward estimator) was initialized as FE_0 , the first iteration of FE_n . FE_n uses the last 1,200 ms of data to make walking speed estimates every 20 ms (50 Hz). These estimates are used to scale ankle push-off and knee swing prosthetic assistance. Every third prosthesis stride, a backward estimator labels the previous strides of prosthesis data. Stride data includes 28 sensor channels from joint encoders, inertial measurement units, and a 6-DOF load cell. Labeled stride data is organized by walking speed labels into bins in a first-in-first-out manner. During adaptation, binned stride data is evenly split into train and validation datasets. A copy FE_0 is re-trained with the train dataset to create an adapted forward estimator (AFE). The AFE and FE_n are evaluated on the validation dataset. If the AFE achieves a lower mean absolute error, it replaces the FE_n and increments n .

Six subjects from this study were involved in collecting the offline dataset [30]. A unique forward estimator (with optimized hyperparameters) was trained for these six subjects using a subset of the offline dataset ($N=10$) that excluded the test subject. The complete offline dataset ($N=11$) was used to train the forward estimator used for the four new subjects. Each subject's pre-trained forward estimator is considered their baseline forward estimator and denoted as FE_0 . As the system operates, the baseline forward estimator (FE_0) is periodically adapted to the individual's walking patterns with the intention of replacing the forward estimator responsible for real-time speed estimation. Adapted versions of FE_0 are denoted as FE_n , where n represents the number of updates the forward estimator has undergone since the start of the trial. The forward estimator attained at the end of an adaptation trial is denoted as FE_F . FE_n provides real-time speed estimates every 20 ms (50 Hz) using the most recent input sequence of size 28×120 . Estimates are filtered using a Kalman filter [31] with a process noise of $1e-5$ and measurement variance of 0.1.

Backward Estimation: We employed a Direct Integration (DI) and Ground Truth (GT) backward estimator to self-label stride data. Backward estimators labeled data on a stride-by-stride basis due to the DI backward estimator, which can only provide one speed estimate per stride. The segmentation of strides was determined by a swing-to-stance body mass threshold of approximately 20%, detected at the moment of heel contact.

The DI backward estimator calculated a single speed label for each prosthesis stride by dividing the positional displacement between consecutive heel contact events by the time elapsed between these events. Prosthesis foot position was tracked at 100 Hz using a commercial foot tracking

system called the Imuwear [32]. The Imuwear fuses integrated linear accelerations and rotational velocities to compute foot position. Drift is mitigated by assuming a zero-velocity moment during midstance. A center-moving-average filter of length 5 was used to smooth labels between consecutive strides. All data points within a stride were assigned the same DI-computed label as IMU integration only allows for one prediction per stride. The Imuwear is a very high quality IMU and was the best in the field for tracking foot position/distance that we were aware of at the time of the study for tracking accurate step length estimates.

The GT backward estimator assigned each data point within a stride a ground truth value of speed that is closest in timestamp. For trials with treadmill walking, ground truth speed was the actual treadmill speed which is streamed over the ROS network at 50 Hz. For trials with overground walking, ground truth speed was COM speed and was computed post-hoc as it could only be determined offline. The COM was assumed to be located at the center of the subject's pelvis: the average position between right anterior superior iliac spine (RASIS), left anterior superior iliac spine (LASIS), right posterior superior iliac spine (RPSIS), and left posterior superior iliac spine (LPSIS) VICON marker positions.

Labeled stride data were organized and assigned to bins based on the stride's average speed label. These bins were categorized in increments of 0.1 m/s. For example, the first bin contained stride data with an average speed label ranging from 0.0 to 0.1 m/s, the second bin from 0.1 to 0.2 m/s, and the last bin from 1.9 to 2.0 m/s. Each bin was allowed a maximum of 7 strides. A first-in-first-out strategy was employed to maintain only the most recent 7 strides in each bin. This binning strategy was used to ensure that forward estimators

were adapted with multi-speed data, with an even distribution across speeds and also limit the computational load of adaptation. Alternatively, one-shot or unconstrained adaptation may overfit forward estimators to the most recent speed and cause catastrophic forgetting of other speeds during training, which we observed in offline tests during development of the system.

Adaptation: Every third prosthesis stride, a copy of the FE_0 underwent a real-time adaptation process during which it was re-trained using all available binned stride data labeled by either the DI or GT backward estimator (Fig. 2). During this adaptation, 80% of the strides in each bin were designated as training data, and 20% as validation data. This process required a minimum of two strides per bin to ensure at least one stride was available for both training and validation. The training loop used a learning rate of 0.0001, a batch size of 32, an Adam optimizer, a mean squared error loss function, and 2 epochs; these hyperparameters were selected through offline optimization with the offline dataset used to train forward estimators. After training, the adapted FE_0 (AFE) and the FE_n were evaluated on the validation dataset. If the adapted AFE demonstrated a lower mean absolute error (MAE) compared to the FE_n , the model weights of the FE_n were immediately updated to match those of the AFE and n was incremented.

Biomimetic Assistance: A finite-state machine dictated gait phase transitions between early stance (ES), late stance (LS), swing flexion (SF), and swing extension (SE) gait phases during walking. Similar to [17], joint-specific sets of stiffness (k), damping (b), and theta equilibrium (θ_{eq}) impedance parameters were defined for each gait phase. The total number of impedance parameters was 24. Joint torque was computed with Eq. 1:

$$\tau_i = -k_{i,s}(\theta_i - \theta_{eq,i,s}) - b_{i,s}\dot{\theta}_i \quad (1)$$

where τ is the commanded torque, i is the knee or ankle joint, s is the gait phase, θ is the measured joint angle, and $\dot{\theta}$ is the measured joint angle velocity. Impedance parameters and torques were computed every 10 ms (100 Hz). Commanded torques were actuated every 1 ms (1000 Hz) with a PID current controller.

Like [17], late stance ankle stiffness ($k_{ankle,LS}$) was defined as:

$$k_{ankle,LS} = C \times W(0.237 \times \theta_{ankle} + 0.028) \quad (2)$$

where θ_{ankle} is the measured ankle angle, W is the subject's body mass (kg), and C is a dimensionless multiplier. Knee swing flexion ($k_{knee,SF}$) and extension ($k_{knee,SE}$) stiffness were defined as constants. In this study, we wrapped $k_{ankle,LS}$, $k_{knee,SF}$, and $k_{ankle,SE}$ in the following scaling equation:

$$k_{scaled,i,s} = k_{i,s}(1 + a(v - ref)) \quad (3)$$

where v is speed, a is the scaling coefficient, and ref is the reference walking speed of 0.5 m/s. Scaling these specific parameters provided additional ankle push-off and knee swing assistance that enabled the prosthesis to biomimetically adjust with changes in speed.

D. Experimental Protocol

This study asked subjects to participate in a tuning session, treadmill trials, and overground trials. Treadmill trials included 2 benchmark trials, 4 adaptation trials, and 6 forward estimation trials. Overground trials consisted of one adaptation trial and one forward estimation trial. Prosthetic assistance was scaled across all trials using Eq. 3. Two distinct treadmill profiles were used throughout treadmill trials:

Treadmill Speed Profiles:

- Profile 1 (P1): Subjects encountered discrete treadmill speeds in the following sequence: 0.3, 0.5, 0.7, 0.9, 0.8, 0.6, 0.4 m/s. Each speed was maintained for 20 seconds before transitioning to the next speed at an acceleration of 0.1 m/s². The total duration for P1 was approximately 140 seconds.
- Profile 2 (P2): The treadmill speed started at 0.3 m/s, accelerated to 0.9 m/s, and then decelerated back to 0.3 m/s at a rate of 0.1 m/s². The total duration for P2 was approximately 80 seconds.

These profiles were selected to evaluate our methods on both discrete (P1) and continuously changing (P2) walking speed patterns.

Tuning Session: State machine transition and impedance parameters were tuned to the preference of the subject during treadmill walking. Commonly tuned parameters included stance-to-swing body mass threshold (%), $k_{ankle,LS}$ (C), $k_{knee,SF}$ (constant), and $k_{knee,SE}$ (constant). These parameters were tuned at 0.5 m/s. Then, the scaling coefficient (a) of each listed stiffness parameter was tuned at 0.3 and 0.9 m/s. This process was repeated until the subject felt properly assisted at 0.3, 0.5, and 0.9 m/s. This tuning process took about 15-30 minutes to complete.

Treadmill Benchmark Trials: Two benchmark trials were collected to create a test dataset for evaluating the true performance of forward estimators during adaptation. For Trial 1 and Trial 2, subjects walked on P1 and P2, respectively. During these trials, forward estimates were set equal to the actual treadmill speeds streamed over ROS, ensuring accurate scaling of prosthetic assistance. This measure was taken to avoid snowballing disturbances in gait that could affect the reliability of subsequent forward estimations. This challenge is faced head on in all other trials in this study. This test dataset was reserved for post-hoc analysis and was not used to inform adaptation decisions.

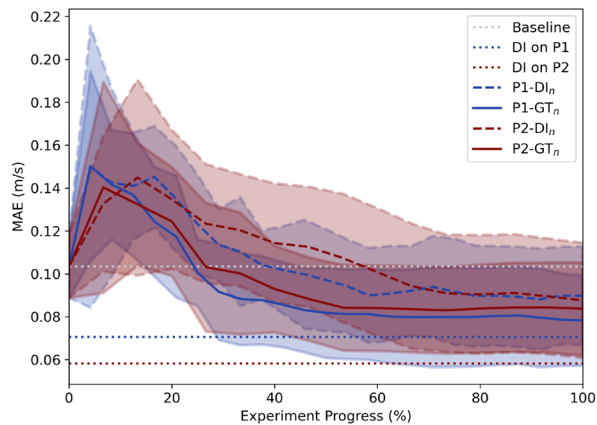


Fig. 3. Walking speed estimation performance of FE_n evaluated on user-dependent test data, collected during benchmark trials. The FE_0 was initialized with a pre-trained, user-independent estimator named the baseline forward estimator. Every third prosthetic stride, a copy of FE_0 was updated with user-dependent data collected and labeled in real-time by a backward estimator (DI or GT) across two treadmill speed profiles (P1 or P2). FE_n is named by the profile and backward estimator used (e.g., P1-DI_n). Results are plotted for each combination of backward estimation and treadmill speed profile. Real-time backward estimation errors are plotted with a red and blue dotted line. Data are averages of multiple subjects with unilateral transfemoral amputation (TF=10) (± 1 SD).

Treadmill Adaptation Trials: Four adaptation trials were collected to adapt the baseline forward estimator (FE_0) to the novel subject under different conditions. An adaptation trial was collected for each unique combination of profile (P1 or P2) and backward estimator (DI or GT). Forward estimation, backward estimation, and adaptation processes were run asynchronously.

A trial-specific naming convention was adopted to track the evolution of adapted forward estimators. This naming scheme incorporated the profile and backward estimator used during the adaptation trial. For example, an adaptation trial using P1 and DI was initialized with a baseline forward estimator named P1-DI₀ (equivalent to FE_0) that evolved as P1-DI_n through adaptation and concluded as an adapted forward estimator named P1-DI_F. Thus, adaptation trials yielded the following adapted forward estimators: P1-DI_F, P1-GT_F, P2-DI_F, and P2-GT_F.

Treadmill Forward Estimation Trials: Six forward estimation trials were collected to assess the real-time speed estimation performance of adapted and non-adapted forward estimators. Only the forward estimation process was run. FE_0 , P1-DI_F, and P1-GT_F were evaluated on P1 in separate trials. FE_0 , P2-DI_F, and P2-GT_F were evaluated on P2 in separate trials.

Overground Adaptation Trial: To evaluate the performance of our methods in a more realistic setting, one adaptation trial was conducted during overground (OVG) walking. Subjects were instructed to walk back and forth along a 5-meter path at their self-selected walking speed for a duration of two minutes. Real-time forward estimates were made with FE_0 . DI backward estimates were recorded for later

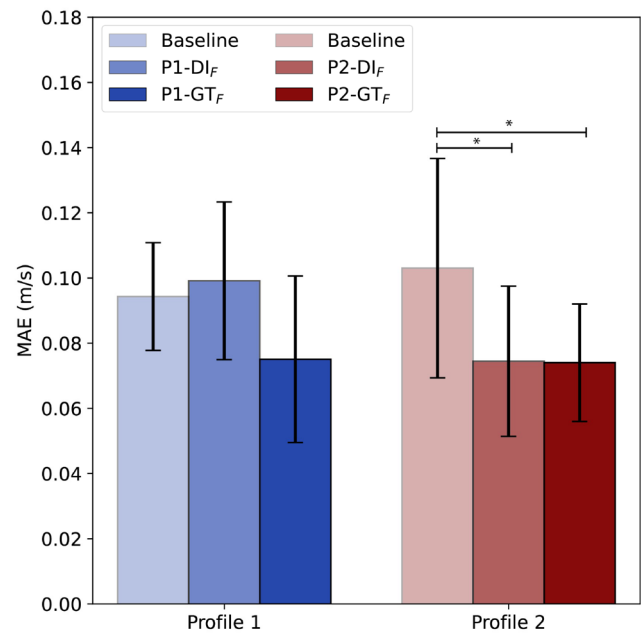


Fig. 4. Real-time forward estimation performance of baseline and final adapted forward estimators on their respective profile (P1 or P2). Data are averages of multiple subjects with unilateral transfemoral amputation (TF=10) (± 1 SD). * denotes statistically significant differences ($p < 0.05$) between estimators, as determined by a repeated measures ANOVA.

use. Due to the lack of real-time GT backward estimates in the overground setting, the adaptation process for this adaptation trial was performed offline with COM speed labels. Offline adaptation yielded the following forward estimators: OVG-DI_F, and OVG-GT_F.

Overground Forward Estimation Trial: One overground forward estimation trial was collected to evaluate the performance of adapted and non-adapted forward estimators in an overground setting. Subjects were given identical walking instructions to the overground adaptation trial. Real-time forward estimates were made with FE_0 . The following forward estimators were evaluated on this trial in an offline manner: FE_0 , P1-DI_F, P1-GT_F, P2-DI_F, P2-GT_F, OVG-DI_F, and OVG-GT_F.

E. Statistical Measurements

A repeated measures ANOVA was conducted to examine the impact of different forward estimators on the real-time forward estimation error, which served as the dependent variable. In this analysis, the forward estimator functioned as the intra-subject factor, with multiple measurements taken for each subject across different conditions. Instances of significant differences were further explored using Tukey's Honest Significant Difference test to conduct detailed comparisons between specific groups.

Paired t-tests were used to compare the offline forward estimation error of each adapted forward estimator with the baseline during overground walking. The error served as the dependent variable in these analyses.

III. RESULTS

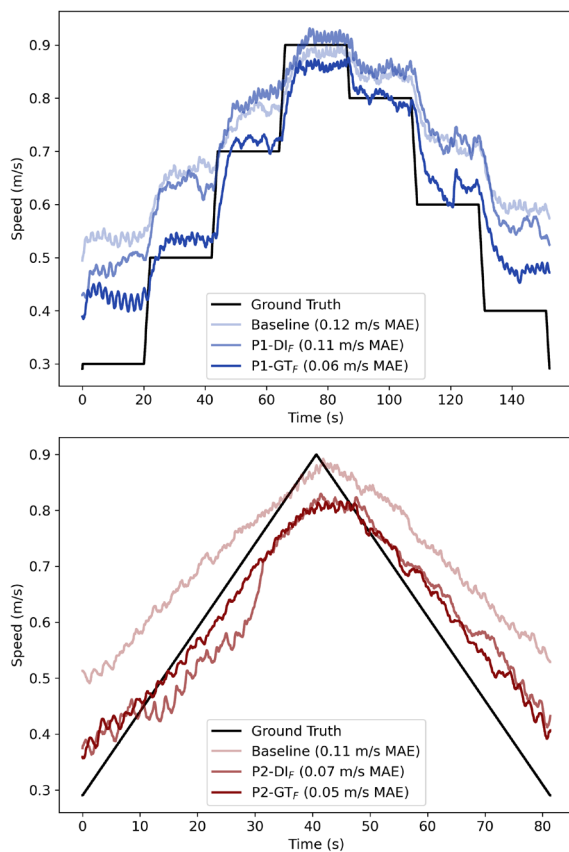


Fig. 5. Real-time forward estimation tracking of baseline forward estimators and adapted forward estimators compared to the ground truth treadmill speeds on treadmill speed profiles P1 (top) and P2 (bottom) for a representative subject (TF09). The real-time forward estimation tracking illustrates the ability of the estimators to predict walking speed in real-time during treadmill walking. The results shown are for a single representative subject, highlighting individual performance. For the overall performance across all subjects, refer to Fig. 4.

Improvements from the baseline (FE₀) performance (0.104 m/s MAE) were observed for all adapted forward estimators by the end of adaptation trials (Fig. 3). Test errors rose sharply before settling to errors less than the baseline. P1-DI_F, P1-GT_F, P2-DI_F, and P2-GT_F achieved errors of 0.090 [0.023], 0.078 [0.021], 0.088 [0.027], and 0.084 [0.022] m/s MAE, respectively. On P1 and P2, DI backward estimation (Imuwear estimation) had average errors of 0.071 [0.031] and 0.058 [0.021] m/s MAE, respectively.

The real-time forward estimation performance of adapted forward estimators were compared to the baseline in Fig. 4 and 5. On P1, the errors of the FE₀, P1-DI_F, and P1-GT_F were 0.094 [0.017], 0.091 [0.024], and 0.075 [0.026] m/s MAE, respectively. On P2, the errors for FE₀, P2-DI_F, and P2-GT_F were 0.103 [0.033], 0.074 [0.023], and 0.074 [0.018] m/s MAE, respectively. For P2, both P2-DI_F and P2-GT_F achieved errors that were significantly lower than the baseline ($p < 0.05$).

Adapted and non-adapted forward estimators were evaluated offline on two minutes of overground walking. Offline forward estimation errors are shown in Fig. 6. Forward

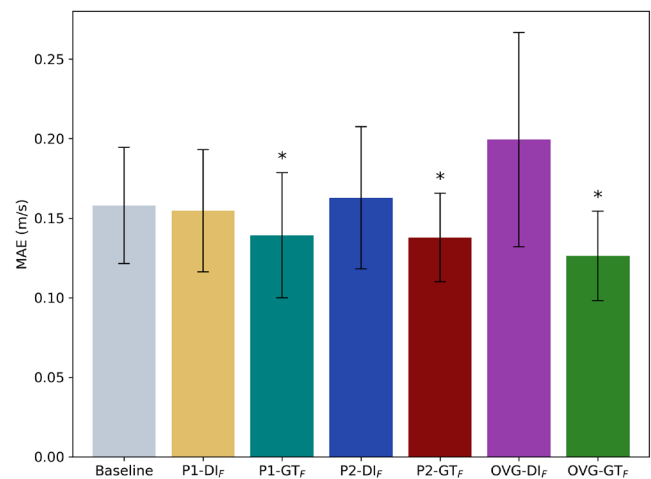


Fig. 6. Offline forward estimation performance of baseline and adapted forward estimators during overground walking. Data are averages of multiple subjects with unilateral transfemoral amputation (TF=10) (± 1 SD). * denotes statistically significant differences ($p < 0.05$) between estimators and the baseline, as determined by multiple paired t-tests.

estimators adapted with the GT backward estimator (P1-GT_F, P2-GT_F, and OVG-GT_F) achieved significantly lower errors (0.139 [0.039], 0.138 [0.028], and 0.126 [0.028] m/s MAE, respectively) compared to the baseline (0.158 [0.037] m/s MAE) ($p < 0.05$). Forward estimators adapted with the DI backward estimator (P1-DI_F, P2-DI_F, and OVG-DI_F) yielded errors of 0.155 [0.038], 0.163 [0.045], and 0.199 [0.067] m/s MAE, respectively.

Prosthesis ankle moment and knee power were compared to able-bodied (AB) biomechanics (N=22) (Fig. 7). For the shared speeds of 0.5, 0.6, 0.7, and 0.8 m/s, a linear fit of peaks was conducted between TF and AB ankle moment and knee power signals. Ankle moment peaks yielded 0.82 and 0.86 N-m/kg/m/s rates for TF and AB subjects, respectively. The Pearson correlation coefficient between ankle moment peaks was 0.91. Knee power peaks yielded 2.2 and 1.2 N-m/kg/m/s rates for TF and AB subjects, respectively. The Pearson correlation coefficient between knee power peaks was also 0.91.

IV. DISCUSSION

The primary goal of this study was to develop a continual learning algorithm for powered lower-limb prostheses that can iteratively improve the performance of forward estimators of speed for novel users. Significant algorithmic changes were made for this regression task compared to adaptation studies involving mode classification [25], [26]. Most notably, we added memory in the form of data bins to avoid catastrophic forgetting, noncausal filtering to smooth sequential backward estimates, and scaling of prosthetic assistance to accommodate changes in speed.

Subjects underwent a series of adaptation trials during which baseline forward estimators were adapted to self-labeled user-dependent data every three strides. We found that adapting at the start of trial, when a limited amount of user-

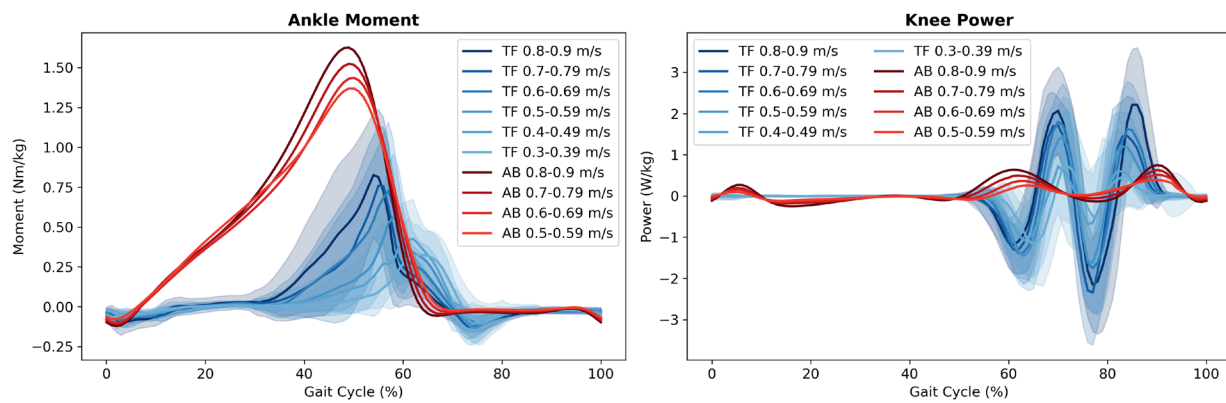


Fig. 7. Cross-subject average ankle moment and knee power from the prosthesis of individuals with transfemoral amputations (TF=10) and the intact limb of able-bodied individuals (AB=22) across speeds. The AB dataset did not contain treadmill walking at speeds below 0.5 m/s. TF biomechanics were taken from benchmark trials during which scaling of assistance was dictated by the ground truth treadmill speed. Prosthesis control parameters were linearly scaled based on speed. Specifically, joint stiffness was linearly scaled during ankle push-off and knee swing extension. The scaling equations were tuned to the preference. The TF biomechanics shown were computed using on-device sensors.

dependent data was available, caused overfitting. Data collected early in the trial contained a narrow distribution of speeds which improved the performance on validation data (i.e., 20% of binned data) but worsened the performance on test data (obtained from benchmark trials). Eventually, all forward estimators achieved test errors that were less than the baseline. P1-GT passed this threshold after 35 sec, P2-GT after 21 sec, P1-DI after 58 sec, and P2-DI after 48 sec. These results suggest that improvements in performance can be attained within a minute of walking given an accurate enough backward estimator. The inability of adapted forward estimators to attain the same error as their respective backward estimators may indicate that there is a limit of improvement for our machine learning approach to forward estimation given that the forward estimation problem is fundamentally harder than backward estimation as less information is available in real-time.

It is interesting to note that the thigh IMU sensor failed during a subject's adaptation trial. Although baseline errors increased initially due to the corrupted sensor data (0.12 MAE m/s), the system was able to adapt and improve upon the baseline (0.10 MAE m/s). While unintended for this study, this accident demonstrated the adaptation system represents a potential solution to handle sensor dropout or corruption for real-time machine learning systems.

Adapted and non-adapted forward estimators were evaluated in real-time on their respective treadmill profile during separate forward estimation trials. Real-time errors (Fig. 4) were not in-line with the test error trends shown in adaptation trials (Fig. 3), but were comparable to speed estimation errors achieved by other studies involving TF subjects [20], [24], [30]. Specifically, P1-DI_F produced a worse real-time error than the baseline (-5%) and P1-GT_F produced a better real-time error than the baseline (20%). Most notably, P2-DI_F (28%) and P2-GT_F (28%) achieved real-time errors that were 1) significantly lower than the baseline and 2) not significantly different from each other. This suggests that adapting to more continuous speeds yields better real-time forward estimation performance. Interestingly,

humans tend to increase and decrease speed much more frequently than they maintain steady-state walking [33], so this finding might be promising for real-world settings. Related adaptation work achieved 7% [26] and 45% [25] improvements in real-time classification accuracy. While not directly comparable, these percentage improvements highlight the potential benefit adaptation can have on real-time inference in prosthetic applications. Our best adaptation performance (28%) may be further improved with longer periods of adaptation, a wider range of speeds, and selective sampling of training data used during adaptation.

Forward estimators adapted with GT labels yielded forward estimation errors that were significantly less than the baseline during overground walking. This result indicates that, given an accurate enough backward estimator, treadmill or overground adaptation can benefit overground forward estimation. Forward estimators adapted with the DI labels yielded errors that were not significantly different from the baseline. The DI backward estimator underperformed possibly due to high accelerations/decelerations in walking speed during overground walking. The maximum change of speed observed during treadmill and overground walking was 0.1 and 0.9 m/s², respectively. The average prosthesis stride duration during treadmill and overground walking was 1.78 [0.24] and 1.92 [0.13] sec, respectively. This meant that, in the worst case, intra-stride speed varied by 0.18 m/s² during treadmill walking and 1.73 m/s² during overground walking, indicating that the accelerations experienced within one stride of overground walking were almost ten times greater than those experienced during treadmill walking. This poses an issue when the DI backward estimators assign the same walking speed label to every data point within one stride. The GT backward estimator had the advantage of assigning labels to individual data points that corresponded to the closest ground truth speed measurement. Future work needs to aim to develop more continuous backward estimators that keep up with rapid intra-stride changes in walking speed or only adapt on data from moments of low acceleration. Direct estimation with IMU, pose, or kinematic approaches that only estimates once

per gait cycle is not only not promising for forward estimation, but is not even sufficient for backward labeling, indicating the importance of machine learning approaches that estimate speed continuously in time. A limitation of this study involved the lack of real-time adaptation and evaluation of forward estimators during overground walking. Future studies should evaluate forward estimators in real-time for longer bouts of walking.

The joint biomechanics shown in Fig. 7 illustrate the scaling effect of our prosthesis controller. By linearly scaling the stiffness impedance parameter during ankle push-off and knee swing based on speed we aimed to better assist subjects during variable-speed walking. A high correlation coefficient (0.91) was achieved in ankle moment and knee power peaks between TF and AB biomechanics. Though we scaled similarly to AB, the magnitudes of ankle moment and knee power were not comparable. Even though our system could predict biomimetic ankle moments, we were unable to fully deliver them at top speeds in a real-time system due to device limitations. Specifically, the ankle joint moment was capped to avoid belt skips within the belt-drive system. This was especially prevalent during ankle push-off when the ankle had to deliver large joint moments to propel the subject’s mass forward. The higher magnitudes of TF knee powers are in part due to user preference tuning. We hypothesize that subjects may have preferred a faster swinging knee to compensate for a lack of ankle push-off propulsion.

V. CONCLUSION

This study introduced a novel real-time continual learning approach for powered lower-limb prostheses that updated a deep-learning-based walking speed estimator with user-dependent data, effectively personalizing the estimator to the user and improving estimation performance over time. Evaluated on ten individuals with transfemoral amputation during treadmill and overground walking, the proposed algorithm demonstrates significant improvements in walking speed estimation, with adapted estimators outperforming the baseline estimator after approximately 1 minute of walking. The results highlight the importance of accurate backward estimators in the adaptation process, the transferability of treadmill adaptation benefits to real-world walking conditions, and the effectiveness of the prosthesis controller in scaling assistance with speed estimates based on biomimetic trends. This study presents a significant step towards developing self-learning prostheses that can adapt to individual users and provide robust and biomechanically appropriate assistance after a short period of walking, ultimately enhancing the quality of life for individuals with lower-limb amputations.

VI. REFERENCES

[1] L. Nolan and A. Lees, “The functional demands on the intact limb during walking for active trans-femoral and trans-tibial amputees,” *Prosthetics and Orthotics International*, vol. 24, no. 2, pp. 117–125, Jan. 2000, doi: 10.1080/03093640008726534.

[2] X. Bonnet, C. Villa, P. Fodé, F. Lavaste, and H. Pillet, “Mechanical work performed by individual limbs of transfemoral amputees during step-to-step transitions: Effect of walking velocity,” *Proc Inst Mech Eng H*, vol. 228, no. 1, pp. 60–66, Jan. 2014, doi: 10.1177/0954411913514036.

[3] L. Nolan, A. Wit, K. Dudziński, A. Lees, M. Lake, and M. Wychowañski, “Adjustments in gait symmetry with walking speed in trans-femoral and trans-tibial amputees,” *Gait & Posture*, vol. 17, no. 2, pp. 142–151, Apr. 2003, doi: 10.1016/S0966-6362(02)00066-8.

[4] E. Russell Esposito, C. A. Rábago, and J. Wilken, “The influence of traumatic transfemoral amputation on metabolic cost across walking speeds,” *Prosthet Orthot Int*, vol. 42, no. 2, pp. 214–222, Apr. 2018, doi: 10.1177/0309364617708649.

[5] R. Gailey, K. Allen, J. Castles, J. Kucharik, and M. Roeder, “Review of secondary physical conditions associated with lower-limb amputation and long-term prosthesis use,” *J Rehabil Res Dev*, vol. 45, no. 1, pp. 15–29, 2008, doi: 10.1682/jrrd.2006.11.0147.

[6] J. Camargo, A. Ramanathan, W. Flanagan, and A. Young, “A comprehensive, open-source dataset of lower limb biomechanics in multiple conditions of stairs, ramps, and level-ground ambulation and transitions,” *Journal of Biomechanics*, vol. 119, p. 110320, Apr. 2021, doi: 10.1016/j.jbiomech.2021.110320.

[7] K. R. Kaufman, S. Frittoli, and C. A. Frigo, “Gait asymmetry of transfemoral amputees using mechanical and microprocessor-controlled prosthetic knees,” *Clinical Biomechanics*, vol. 27, no. 5, pp. 460–465, Jun. 2012, doi: 10.1016/j.clinbiomech.2011.11.011.

[8] A. D. Segal *et al.*, “Kinematic and kinetic comparisons of transfemoral amputee gait using C-Leg and Mauch SNS prosthetic knees,” *JRRD*, vol. 43, no. 7, p. 857, 2006, doi: 10.1682/JRRD.2005.09.0147.

[9] T. Schmalz, S. Blumentritt, and B. Marx, “Biomechanical analysis of stair ambulation in lower limb amputees,” *Gait & Posture*, vol. 25, no. 2, pp. 267–278, Feb. 2007, doi: 10.1016/j.gaitpost.2006.04.008.

[10] A. F. Azocar, L. M. Mooney, L. J. Hargrove, and E. J. Rouse, “Design and Characterization of an Open-Source Robotic Leg Prosthesis,” in *2018 7th IEEE International Conference on Biomedical Robotics and Biomechatronics (Biorob)*, Aug. 2018, pp. 111–118, doi: 10.1109/BIOROB.2018.8488057.

[11] L. M. Sullivan, S. Creveling, M. Cowan, L. Gabert, and T. Lenzi, “Powered Knee and Ankle Prosthesis Control for Adaptive Ambulation at Variable Speeds, Inclines, and Uneven Terrains,” in *2023 IEEE/RSJ International Conference on Intelligent Robots and Systems (IROS)*, Oct. 2023, pp. 2128–2133, doi: 10.1109/IROS55552.2023.10342504.

[12] B. E. Lawson, J. Mitchell, D. Truex, A. Shultz, E. Ledoux, and M. Goldfarb, “A Robotic Leg Prosthesis: Design, Control, and Implementation,” *IEEE Robotics*

- 1 & *Automation Magazine*, vol. 21, no. 4, pp. 70–81, Dec.
2 2014, doi: 10.1109/MRA.2014.2360303.
- 3 [13] T. Elery, S. Rezazadeh, C. Nesler, and R. D. Gregg,
4 “Design and Validation of a Powered Knee-Ankle
5 Prosthesis with High-Torque, Low-Impedance
6 Actuators,” *IEEE Trans Robot*, vol. 36, no. 6, pp. 1649–
7 1668, Dec. 2020, doi: 10.1109/TRO.2020.3005533.
- 8 [14] T. K. Best, C. G. Welker, E. J. Rouse, and R. D. Gregg,
9 “Data-Driven Variable Impedance Control of a Powered
10 Knee–Ankle Prosthesis for Adaptive Speed and Incline
11 Walking,” *IEEE Transactions on Robotics*, pp. 1–19,
12 2023, doi: 10.1109/TRO.2022.3226887.
- 13 [15] T. Lenzi, L. Hargrove, and J. Sensinger, “Speed-
14 Adaptation Mechanism: Robotic Prostheses Can
15 Actively Regulate Joint Torque,” *IEEE Robotics &
16 Automation Magazine*, vol. 21, no. 4, pp. 94–107, Dec.
17 2014, doi: 10.1109/MRA.2014.2360305.
- 18 [16] F. Sup, H. A. Varol, J. Mitchell, T. Withrow, and M.
19 Goldfarb, “Design and control of an active electrical
20 knee and ankle prosthesis,” in *2008 2nd IEEE RAS &
21 EMBS International Conference on Biomedical
22 Robotics and Biomechatronics*, Oct. 2008, pp. 523–528.
23 doi: 10.1109/BIOROB.2008.4762811.
- 24 [17] A. M. Simon *et al.*, “Configuring a Powered Knee and
25 Ankle Prosthesis for Transfemoral Amputees within
26 Five Specific Ambulation Modes,” *PLOS ONE*, vol. 9,
27 no. 6, p. e99387, Jun. 2014, doi:
28 10.1371/journal.pone.0099387.
- 29 [18] A. M. Sabatini, C. Martelloni, S. Scapellato, and F.
30 Cavallo, “Assessment of walking features from foot
31 inertial sensing,” *IEEE Transactions on Biomedical
32 Engineering*, vol. 52, no. 3, pp. 486–494, Mar. 2005,
33 doi: 10.1109/TBME.2004.840727.
- 34 [19] Q. Li, M. Young, V. Naing, and J. M. Donelan,
35 “Walking speed and slope estimation using shank-
36 mounted inertial measurement units,” in *2009 IEEE
37 International Conference on Rehabilitation Robotics*,
38 Jun. 2009, pp. 839–844. doi:
39 10.1109/ICORR.2009.5209598.
- 40 [20] B. Dauriac, X. Bonnet, H. Pillet, and F. Lavaste,
41 “Estimation of the walking speed of individuals with
42 transfemoral amputation from a single prosthetic shank-
43 mounted IMU,” *Proc Inst Mech Eng H*, vol. 233, no. 9,
44 pp. 931–937, Sep. 2019, doi:
45 10.1177/0954411919858468.
- 46 [21] Y. Liu, H. An, H. Ma, and Q. Wei, “Online Walking
47 Speed Estimation Based on Gait Phase and Kinematic
48 Model for Intelligent Lower-Limb Prosthesis,” *Applied
49 Sciences*, vol. 13, no. 3, Art. no. 3, Jan. 2023, doi:
50 10.3390/app13031893.
- 51 [22] K. Bhakta, J. Camargo, W. Compton, K. Herrin, and A.
52 Young, “Evaluation of Continuous Walking Speed
53 Determination Algorithms and Embedded Sensors for a
54 Powered Knee and Ankle Prosthesis,” *IEEE Robotics
55 and Automation Letters*, vol. 6, no. 3, pp. 4820–4826,
56 Jul. 2021, doi: 10.1109/LRA.2021.3068711.
- 57 [23] A. J. Young and L. J. Hargrove, “A Classification
58 Method for User-Independent Intent Recognition for
59 Transfemoral Amputees Using Powered Lower Limb
60 Prostheses,” *IEEE Trans Neural Syst Rehabil Eng*, vol.
24, no. 2, pp. 217–225, Feb. 2016, doi:
10.1109/TNSRE.2015.2412461.
- [24] K. Bhakta, J. Camargo, L. Donovan, K. Herrin, and A.
Young, “Machine Learning Model Comparisons of User
Independent & Dependent Intent Recognition Systems
for Powered Prostheses,” *IEEE Robot. Autom. Lett.*, vol.
5, no. 4, pp. 5393–5400, Oct. 2020, doi:
10.1109/LRA.2020.3007480.
- [25] R. B. Woodward, A. M. Simon, E. A. Seyforth, and L.
J. Hargrove, “Real-Time Adaptation of an Artificial
Neural Network for Transfemoral Amputees Using a
Powered Prosthesis,” *IEEE Trans Biomed Eng*, vol. 69,
no. 3, pp. 1202–1211, Mar. 2022, doi:
10.1109/TBME.2021.3120616.
- [26] J. A. Spanias, A. M. Simon, S. B. Finucane, E. J.
Perreault, and L. J. Hargrove, “Online adaptive neural
control of a robotic lower limb prosthesis,” *J. Neural
Eng.*, vol. 15, no. 1, p. 016015, Jan. 2018, doi:
10.1088/1741-2552/aa92a8.
- [27] C. Johnson, J. Cho, J. Maldonado-Contreras, S.
Chaluvadi, and A. J. Young, “Adaptive Lower-Limb
Prosthetic Control: Towards Personalized Intent
Recognition & Context Estimation,” in *2023
International Symposium on Medical Robotics (ISMR)*,
Atlanta, GA, USA: IEEE, Apr. 2023, pp. 1–7. doi:
10.1109/ISMR57123.2023.10130251.
- [28] C. Lea, R. Vidal, A. Reiter, and G. D. Hager, “Temporal
Convolutional Networks: A Unified Approach to Action
Segmentation.” arXiv, Aug. 29, 2016. doi:
10.48550/arXiv.1608.08242.
- [29] D. D. Molinaro, I. Kang, J. Camargo, M. C. Gombolay,
and A. J. Young, “Subject-Independent, Biological Hip
Moment Estimation During Multimodal Overground
Ambulation Using Deep Learning,” *IEEE Trans. Med.
Robot. Bionics*, vol. 4, no. 1, pp. 219–229, Feb. 2022,
doi: 10.1109/TMRB.2022.3144025.
- [30] “Multi-Context, User-Independent, Real-Time Intent
Recognition for Powered Lower-Limb Prostheses.”
Accessed: Apr. 02, 2024. [Online]. Available:
<https://repository.gatech.edu/entities/publication/10ac62bd-e44c-4554-b7cd-1b73c4e0412f>
- [31] R. E. Kalman, “A New Approach to Linear Filtering
and Prediction Problems,” *Journal of Basic
Engineering*, vol. 82, no. 1, pp. 35–45, Mar. 1960, doi:
10.1115/1.3662552.
- [32] L. Ojeda and J. Borenstein, “Non-GPS Navigation for
Security Personnel and First Responders,” *The Journal
of Navigation*, vol. 60, no. 3, pp. 391–407, Sep. 2007,
doi: 10.1017/S0373463307004286.
- [33] M. S. Orendurff, J. A. Schoen, G. C. Bernatz, A. D.
Segal, and G. K. Klute, “How humans walk: bout
duration, steps per bout, and rest duration,” *J Rehabil
Res Dev*, vol. 45, no. 7, pp. 1077–1089, 2008, doi:
10.1682/jrrd.2007.11.0197.



Jairo Y. Maldonado-Contreras received a B.S. degree in Mechanical Engineering from California State University Long Beach in 2019. He is currently a Robotics Ph.D. candidate at Georgia Institute of Technology. His interests include wearable robots, autonomous robots, and artificial intelligence.



Cole Johnson received a B.S. degree in Computer Science: Intelligence & Theory from and is currently a Computational Perception & Robotics M.S. student at Georgia Institute of Technology. His interests include autonomous robotics, specifically at the intersection of controls and ML.



Sixu Zhou received a B.S. in Mechanical Engineering from The University of Texas at Arlington and a M.S. in Mechanical Engineering from Georgia Institute of Technology in 2020 and 2022, respectively. He is currently a Robotics Ph.D. student at Georgia Institute of Technology. His interests include wearable robots, biomechatronics, and robot control.



Hanjun Kim received a B.S. degree in Operational Research from Korea Military Academy in 2014, and M.S. degree in Mechanical Engineering from Purdue University in 2019. He is currently a Mechanical Engineering Ph.D. student at Georgia Institute of Technology. His interests include artificial intelligence, smart robots, and human-robot interaction.



Ian Knight is pursuing a B.S. degree in Computer Science at Georgia Institute of Technology. His interests include autonomous robotics and machine learning.



Kinsey R. Herrin received a B.S. in Chemistry from the University of Georgia and a M.S. in Orthotics and Prosthetics from Georgia Institute of Technology in 2008 and 2010, respectively. She is currently a Senior Research Scientist at Georgia Institute of Technology. Her interests include rehabilitative technology, human-robot interaction, and patient care.



Aaron J. Young received a B.S. in Biomedical Engineering from Purdue University and a Ph.D. in Biomedical Engineering from Northwestern University in 2009 and 2014, respectively. He is an Associate Professor at Georgia Institute of Technology. His research interests include wearable robotics, machine learning, and human biomechanics.